International Journal of Electrical and Computer Engineering (IJECE)
Vol. 15, No. 5, October 2025, pp. 4465~4476
ISSN: 2088-8708, DOI: 10.11591/ijece.v15i5.pp4465-4476

Design of a solar-powered electric vehicle charging station

Emerson Cabanzo Mosquera, Walter Naranjo Lourido, Javier Eduardo Martínez Baquero
Engineering School, Faculty of Basic Sciences and Engineering, Universidad de los Llanos, Villavicencio, Colombia

Article Info

Article history:

Received Feb 12, 2025
Revised May 29, 2025
Accepted Jul 3, 2025

Keywords:

Battery storage system
Charging station
Photovoltaic system
Renewable energy
Solar-powered infrastructure
Sustainability

ABSTRACT

This manuscript presents the design of a solar-powered electric vehicle (EV) charging station in Villavicencio, Colombia, aimed at reducing reliance on the utility grid, lowering energy costs, and minimizing environmental impact. The station designed integrates a photovoltaic system to harness renewable energy, ensuring a sustainable and cost-effective charging solution. It accommodates both AC and DC fast charging options to meet diverse vehicle requirements. The design considers available space, energy generation potential, and financial feasibility to maximize efficiency and return on investment. A technical analysis of battery storage, power electronics, and system configuration is provided, along with a cost-benefit assessment. Simulation results confirm the station's ability to deliver stable power under varying conditions. With an estimated payback period of 2.8 years, this project demonstrates the economic and environmental advantages of solar-powered EV infrastructure, supporting the transition to clean transportation in Colombia.

Corresponding Author:

Javier Eduardo Martinez Baquero
Engineering School, Faculty of Basic Sciences and Engineering, Universidad de Los Llanos
Transversal 25 #13-34. Villavicencio, Colombia
Email: jmartinez@unillanos.edu.co

1. INTRODUCTION

Greenhouse gas concentrations in the atmosphere are steadily rising due to human activities, significantly impacting the climate system [1]–[3]. Key contributors include industrial production processes and fuel combustion, which generate emissions that accelerate climate change. The widespread use of electronic devices such as smartphones, computers, and televisions has significantly increased energy consumption and carbon emissions, reporting a 53% rise in greenhouse gas emissions from electronic devices and e-waste between 2014 and 2020, further accelerating global warming and its severe environmental consequences [4], [5].

Combustion engine vehicles are a significant source of pollution, emitting carbon dioxide into the atmosphere [6], [7]. Alongside other human activities, these emissions intensify the greenhouse effect, leading to rising global temperatures, extreme weather conditions, and severe environmental degradation [8], [9]. A shift to cleaner energy sources such as solar, wind, and hydroelectric power is essential. Equally important is promoting sustainable consumption habits, such as improving energy efficiency and reducing waste, to lower carbon footprints. The development and widespread adoption of eco-friendly transportation solutions, including electric vehicles and improved public transit systems, will further reduce emissions. Governments, industries, and individuals must prioritize policies that accelerate clean energy adoption and invest in carbon-neutral technologies. By taking proactive steps, like ending fossil fuel subsidies and expanding renewable energy grids, society can mitigate climate change and work toward a more sustainable and resilient planet [10], [11].

The impact of greenhouse gas emissions has driven industries and consumers to adopt innovative strategies that enhance production, consumption and waste management processes. These advancements do not only improve efficiency but also reduce environmental harm by lowering carbon footprints. To mitigate emissions, industries are integrating cutting-edge technologies such as carbon capture systems and energy-efficient transportation solutions. For example, the maritime sector is transitioning to cleaner propulsion methods, including liquefied natural gas (LNG) and electric-powered ships, which significantly decrease CO_2 and sulfur emissions. Such innovations play a crucial role in reducing the environmental impact of industrial activities and promoting sustainable development [12]–[14].

Transportation accounts for over 25% of global carbon dioxide (CO_2) emissions from internal combustion engine vehicles [15], [16]. As technological advancements, electric vehicle (EV) adoption continues to rise. To support this shift, global research efforts are focused on advancing electric vehicles, battery technologies, and renewable energy sources for charging infrastructure. To accelerate this transition, worldwide electrification efforts must replace the entire fleet of internal combustion engine vehicles (ICEVs) with electric alternatives. Given their lower emissions, electric vehicles play a key role in reducing the global carbon footprint [17], [18]. "In June, Colombia's Single National Traffic Registry (RUNT) reported 8,299 electric vehicles, an increase of 1,891 units in just six months. This trend highlights the growing adoption of EV technology [19]. According to Figure 1, approximately 30% of EV in Colombia are automobiles, making the principal customers for the design of the electric station. Data from the Ministry of Transportation shows that 95% of the country's electric vehicles are concentrated in five regions, with Bogotá DC alone accounting for 47%, as shown in Figure 2.

Figure 1. Classification of electric vehicles by type in Colombia [19]

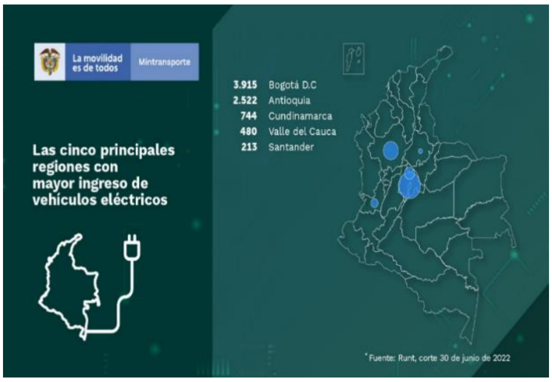

Figure 2. Geographic distribution of electric vehicles in Colombia [19]

Colombia does not have enough charging stations to cover current or future demand. The country has only 173 stations, with 38 in Bogotá DC and 23 in Medellín [20]. Many cities and municipalities lack any charging infrastructure, making EV adoption difficult. To solve this, new fast and cost-efficient charging stations must be built. Law 1964 of 2019 requires municipalities, except Buenaventura and Tumaco, to install at least five fast-charging stations within three years of the law's enactment. It also allows public-private partnerships to fund and build this infrastructure [21]. Expanding charging stations is not just necessary, it is legally required.

Villavicencio was selected for this study because it is an intermediate city, regarding population, with only one charging station. To comply with Law 1964, the city must accommodate from 20 to 50 EVs, meaning multiple new stations are needed. With EV numbers expected to rise due to the global energy transition, the demand for charging stations will only grow. The cost of electricity in Villavicencio depends on contracted load, not usage hours or supply voltage [22]. A solar-powered charging station can lower costs by reducing grid dependency. Meta Electrification Company (EMSA), the regional energy provider, sets pricing for feasibility studies, transformers, and other necessary equipment, all of which must be considered when designing the station.

The article is structured in four sections, the first section (introduction) describes the state of the art. The second section presents the methods and materials used. The third section analyses the results and finally the fourth section presents the conclusions reached. This exploration projects relevant to future research in each are involved.

2. METHOD

To design the electric station [23]–[25], the five most widely sold electric vehicles in the country were selected, as shown in Table 1. This table highlights key characteristics such as energy consumption, driving range, and charging requirements. For the design of the electric station, the characteristics of the electric vehicles to which the charging service will be provided must be considered. In this case, the design will be based on the previously mentioned vehicles [26], [27]. This includes selecting the appropriate battery system, photovoltaic panels, inverter, maximum power point tracking (MPPT) controllers, cables, and other essential components. The station's capacity and peak power output must be determined based on these vehicle specifications [28], [29].

Table 1. Electric vehicle specifications

Vehicle	Battery	Autonomy (Km)	Type of load	Power	Charging time (hours)
RENAULT TWIZY	60 V 8 kWh	80	110 VAC	---	6
RENAULT ZOE E-TECH	400 V 52 kWh	377	DC 110 VAC 110 VAC 110 VAC	50 kW 22 kW 11 kW 3.7 kW	1.05 2.15 4.3 14.58
AUTECO DONGFENG RICH 6EV	385 V 67 kWh	400 (regenerative braking)	200 VAC	6.6 kW	8 to 10
BYD i DOLPHIN	44.9 kWh	400	DC AC	50 kW 5.6 kW	1 8
BYD TANG EV	640 V 86.4 kWh	500	AC DC	5.6 kW 110 kW	15.3 1.2

The first step in the design process is to determine the number of charging points needed to serve multiple vehicles simultaneously [30]. In this case, the station will include six fast-charging points (DC voltage) and two slow-charging points (AC voltage) [31], [32]. The second step is defining the power capacity for each charger. Since Renault Twizy does not specify its charging power in the datasheet, an estimation was made based on similar AC-charged vehicles. Using power-time interpolation, Twizy's charging power is calculated at 6.93 kW.

The total power requirement of the charging station is then established. Assuming a peak demand of 110 kW per vehicle, the station must supply a total of 660 kW when all chargers are in use. In case of a power failure, the design ensures that half of the peak power (330 kW) is delivered from backup battery storage. To accommodate the BYD Tang, which requires 110 kW, the vehicle's 86,4 kWh battery capacity is multiplied by six to determine the total power requirement when all vehicles are charging simultaneously, resulting in 518.4 kWh. Based on this energy demand, the UU 12-200 battery was selected, as detailed in Table 2. The total number of batteries needed is calculated by dividing half of the total power demand by the capacity of each selected battery (2,56 kWh), as shown in (1).

$$No_{batteries} = 101.25 \approx 100 \tag{1}$$

Table 2. Battery characteristics

Characteristic	Value
Standard capacity	200 Ah/12.8 V
Solar panel charging voltage	22 V
Maximum operating current	100 A
Storage capacity	2.56 kWh

Based on equation (1), 100 batteries are required to supply half of the total charging demand for six BYD Tang vehicles. The number of batteries in series is determined by dividing the vehicle's battery voltage by the voltage of the selected battery, while the number of batteries in parallel is calculated by dividing the total required current by the rated current of a single battery. According to (2) and (3), the final battery configuration is 50S2P, ensuring a total output of 640 V, which meets the charging requirements for the BYD Tang.

$$No_{batteries\ in\ series} = 50 \tag{2}$$

$$No_{batteries\ in\ parallel} = 2 \tag{3}$$

On the other hand, given an estimated area of 1,200 m² for the electric station, the number of MONOCRYSTALLINE JMPV-T7/66 (705–715W) photovoltaic panels that can be installed to charge the batteries is determined based on the technical specifications outlined in Table 3. To determine the number of photovoltaic panels that can be installed in the electric station, the area occupied by a single panel must be calculated using its dimensions (Length × Width). The panel's area is provided in (4).

$$A_{Panel} = 3.106\ m^2 \tag{4}$$

Table 3. Technical characteristics of photovoltaic panels

Characteristic	Value
Peak Power	715 W_p
Open circuit voltage	47.24 VDC
Short circuit current	19.25 A
Efficiency	23.02%
Weight	33.4 Kg
Dimensions	(2384 × 1303 × 35) mm

Photovoltaic panels will be installed on the roof of the waiting area of the electric station, as well as on the protective roofing of each electric vehicle charging station, covering an estimated area of 800 m². The total number of panels that can be installed is determined by dividing the available installation area by the area occupied by a single panel, as shown in (5). Based on the number of installed panels, the maximum power output for the electric station is calculated using (6), getting $184.47\ kW_p$.

$$No_{Panels} = 257.5\ \approx 258 \tag{5}$$

$$P_{panels} = No_{Panels} * \text{ Panel peak power} \tag{6}$$

Taking into account the data obtained from the selected battery, the MPPT SR-MC48100N25 will be used which has the following characteristics shown in Table 4. To maximize the voltage and current available for charging the batteries while staying within the MPPT limits, the panel distribution must be carefully designed. Equation (7) is used to determine the number of panels connected in series.

Table 4. Technical characteristics of battery

Characteristic	Value
Maximum input voltage of the panels	250 V
Charge current	100 A
System voltage	12 V/24 V/36 V/48 V

$$No_{panels\ in\ series} = \frac{\text{maximum input voltage}}{\text{panel's open circuit voltage}} = 5.29 \tag{7}$$

With the result obtained in (6), the voltage generated with the connection of the panels in series will be calculated as shown in (8). Voltage of the panels connected in series will not exceed the maximum voltage supported by the MPPT. The number of panels in parallel is defined as shown in (9) and current of the parallel connection is 96.25 A.

$$V_{panels\ in\ series} = 236.2\ VDC \tag{8}$$

$$No_{panels\ in\ parallel} = \frac{\text{maximum load current}}{\text{short circuit current of the panel}} = 5.1 \tag{9}$$

According to calculated current, the amperage of the panels connected in parallel remains within the maximum current limit supported by the MPPT. Considering the MPPT specifications and the number of photovoltaic panels, one MPPT will be installed for each 5S5P array, requiring a total of 10 MPPTs to connect 250 photovoltaic panels. Additionally, an extra MPPT is needed for a 5S2P arrangement to ensure that the voltage generated by the series-connected panels remains consistent with other configurations, preventing circulating currents. As a result, two additional solar panels will be installed, increasing the total to 260 panels. This adjustment requires a recalculation of the installation area, as shown in (10).

$$A_{panels} = 807.56\ m^2 \quad (10)$$

Considering the photovoltaic panels' specifications, the protection diode against circulating currents and the cable gauge for connecting the photovoltaic panels to the MPPT must be carefully selected to ensure system efficiency and safety. According to the photovoltaic panel specifications, the VS-SD403C08S10C diode is chosen for protection against circulating currents. This diode has a reverse voltage (RV) of 800 V and a forward current (IF) of 430 A, making it suitable for the photovoltaic system.

The conductor cable used to interconnect the photovoltaic panels with the MPPT and the 50S2P battery array must be capable of handling the system's maximum current. A No. 2 THHN/THWN 90°C cable is selected, which can carry up to 130 A. This cable selection includes a 30% oversizing margin, preventing excessive heat dissipation. Additionally, the cable's diameter and weight (Kg/km) are within acceptable limits, considering that the total connection length within the electric station does not exceed 100 meters.

The three-phase transformer selection is determined by the total power demand of the battery system, as this represents the peak power required for charging electric vehicles. A 1,000 kVA, 13,200 V three-phase transformer is selected to manage approximately 800 kW, providing a 20% power oversizing margin to enhance reliability. The transformer's amperage must be calculated to define the appropriate conductor gauge, as outlined in (11).

$$I_{Transformer} = \frac{1{,}000\ kVA * 1{,}000}{1.73 * 13{,}200\ V} = 43.79\ A \quad (11)$$

According to (10) it is defined that the conductor must be capable of conducting 44 A, for which the No. 6 gauge of the THHN/THWN 90 °C cable is capable of conducting, causing an oversizing of 60%, which ensures that it will not dissipate excess heat, which would generate losses. For the rectification of the AC voltage that is generated from the transformer, the NTE6030 diode will be used, it is VRRM=300 V, RV=240V and IF=60A.

The BUCK-BOOST circuit will be in charge of regulating the voltage at the output of the 50S2P battery array that will charge electric vehicles; the circuit is made up of an inductor, a capacitor, a diode, and two IGBTs; it also has a closed-loop control for the generation of the PWM towards the IGBTs. In order to define the values of the components, the duty cycle of the DC/DC converter must be calculated, which is calculated by dividing the output voltage of the converter and the sum of the output voltage by the voltage that will provide the battery array (0.75 V to 0.86 V), since a closed-loop control will be carried out, the Duty Cycle value will vary as required by the system. The selected IGBT is the IXYK140N90C3 has Vecs=900 V and Ic=140 A.

The selection of the capacitor is based on the calculation of the resistance produced by the vehicle that will be charged (BYD TANG), whose approximate value is 2.7 Ω; this resistance value is multiplied by the difference of 1 and the Duty Cycle and then divided by two times the working frequency of the PWM (10,000 Hz), so the value that the capacitor must have been 2.646 µF. The ECW-FG80275J capacitor is 0.27 µF and Vdc=800 V.

The selection of the inductor is calculated through the division between the duty cycle and the multiplication of the resistance of the vehicle by the frequency and the percentage of tolerance (1%), so the value that the inductor must have been 3.18 µH. Inductor NR3010T3R3M is 3.5 µH and Idc max=940 A. The selected DC/DC converter to regulate the voltage the transformer rectification provides is the MW1000-DD15-P, which has the characteristics shown in Table 5.

Table 5. DC/DC converter characteristics

Characteristic	Value
Vin	60 – 145 VDC
Vout	120 – 240 VAC
Frequency	50 – 60 Hz

3. RESULTS AND DISCUSSION

Figure 3 shows the circuit diagram designed for the electric station, which incorporates the previously photovoltaic panel arrangements. To prevent circulating currents, a series diode is placed between strings in parallel, as depicted in Figure 4. Also, the battery arrangement is connected to a DC/DC converter, which regulates the DC charging voltages for different vehicles. Additionally, the transformer connected to the distributer electrical network (EMSA) undergoes rectification using a diode per phase. After rectification, the output is fed into a DC/DC converter that regulates the battery charging voltage. When full power is not being used for vehicle charging, the 50S2P battery system stores excess energy. Furthermore, a second connection from the DC/DC converter is linked to an inverter, supplying power to the two AC charging points.

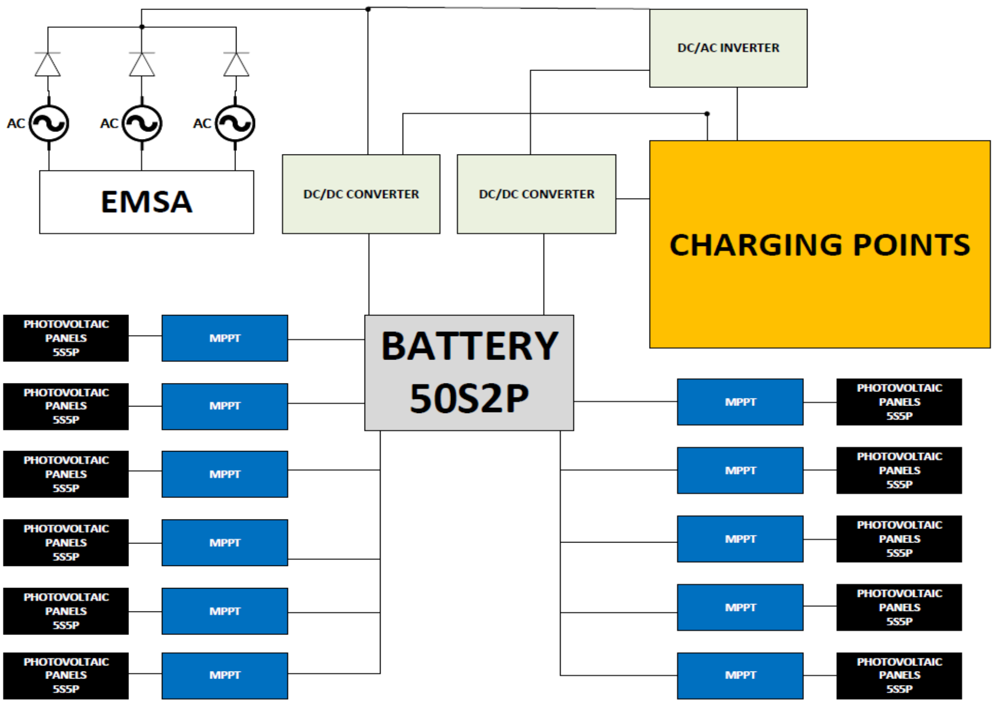

Figure 3. Electric station circuit diagram

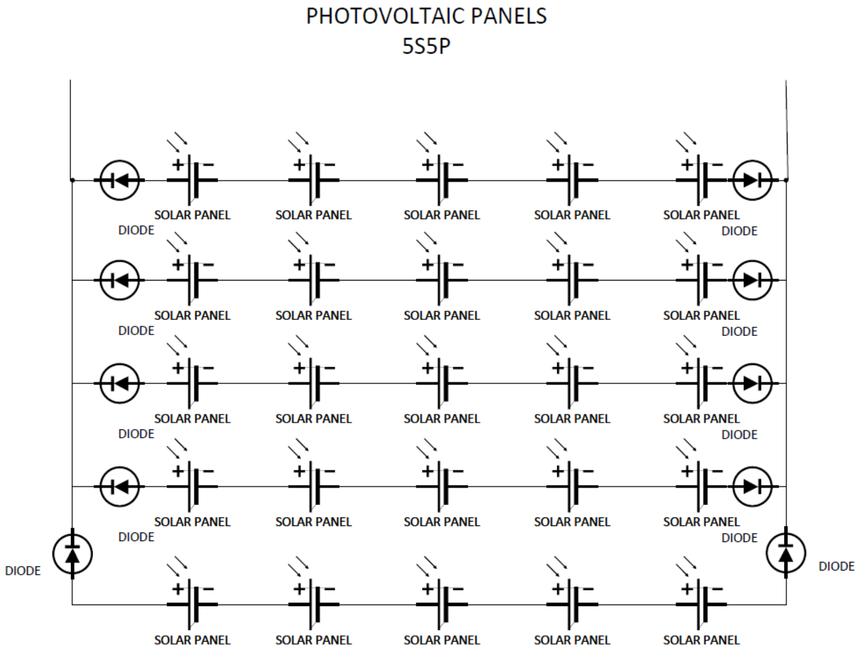

Figure 4. 5S5P system of photovoltaic panels

Figure 5 shows the circuit designed for the BUCK-BOOST type DC/DC converter, from which the charging of electric vehicles will be carried out). The reason why the converter has two IGBTs is that the output voltage of the converter is non-inverting and Table 6 establishes the cost and quantity of equipment and components necessary for the design of the charging station.

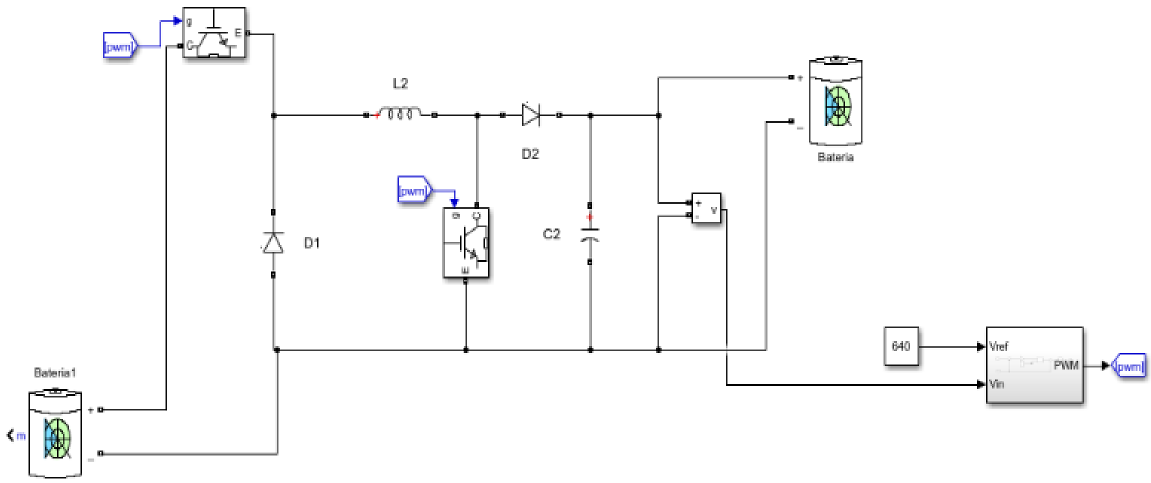

Figure 5. DC/DC converter for vehicle charging from the battery pack

Table 6. Equipment and component costs for the power station

Material	Unit Cost (COP)	Amount (COP)	Total Cost (COP)
12 V 200Ah lithium battery	2´460,000	100	246´000,000
JMPV-T7/66-705-715® Monocrystalline Solar Panel	928,664	260	241´452,645
MPPT MC48100N25	2´639,130	11	29´030,430
Diode VS-SD403C08S10C	321,893	12	3´862,716
Insulated Copper Wire No 6 AWG THHN Color Black Meter	9,700	1,000	9´700,000
Insulated Copper Wire No 2 AWG THHN Color Black Meter	23,400	1,000	23´400,000
ABB transformer 13200 V 1000 KVA	207´773,995	1	207´773,995
Diode NTE6030	74,562	3	223,686
Capacitor ECW-FG80275J	17,693	1	17,693
IGBT IXYK140N90C3	111,486	2	222,972
Inductor NR3010T3R3M	2,061	1	2,061
GS12K ZLPOWER inverter	9´287,000	1	9´287,000
DC/DC converter MW1000-DD15-P	2´022,649	1	2´022,649
Total		772´995,851	

Considering the costs for the design of the electric station, the time necessary to recover the money that will be invested will be estimated; for this, the power generated by the 260 panels is according to (12). Given the power generated in (11), photovoltaic panels generate power in one day according to (13), getting $1154.4\ kWh/day$ and power in one year is calculated using (14), getting 407.12 MWh/year.

$$P_{panels} = 185.9\ kW_p \tag{12}$$

$$P_{day} = 185.9\ kW_p * 6\ h \tag{13}$$

$$P_{year} = \frac{(1154.4\ kWh * 365\ días)}{1000} \tag{14}$$

Assuming that EMSA will charge the utility COP 675 per kWh, time required for the amount of kWh generated by photovoltaic panels in one year to begin to generate profits in terms of consumption and energy cost will be calculated using (15), getting $COP\ 274´806{,}675$. This way, return in obtained according to (16), it is estimated that approximately 2 years, 9 months, and 3 weeks are required to obtain the full return on the investment made. Therefore, from that date, the photovoltaic panels will increase the economic gain of the charging station.

$$Annual_{Return} = (407.121MWh/year * 1{,}000) * 675 \quad (15)$$

$$Total_{Return} = \frac{772'995{,}851\ COP}{274'806{,}675\ COP} \quad (16)$$

Figure 6 shows the charging system designed for the battery arrangement of the electric station. The photovoltaic panel array follows a 5S5P configuration, as it is connected to the MPPT system. The MPPT system and passive components (resistor-capacitor circuit, diode, inductor and capacitor) represent the internal circuits of the SR-MC48100N2. The battery arrangement in the figure is shown as 5S2P, whereas the original 50S2P configuration is designed to charge six vehicles simultaneously. This smaller 5S2P setup is used to simulate the charging process for a single vehicle.

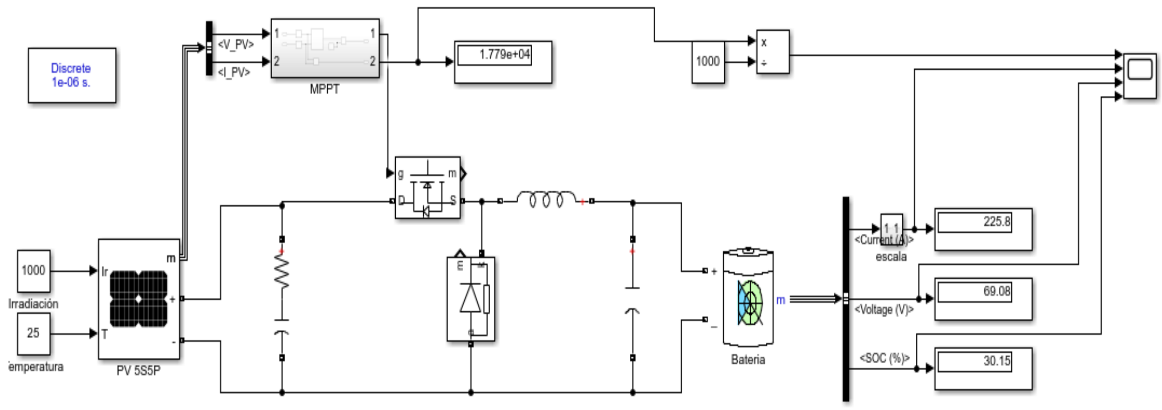

Figure 6. Battery array charging system simulation

Figure 7 shows the power and current generated by the 5S5P panel arrangement when the solar irradiation per square meter varies. The irradiance varies due to the sun's position during the day, the weather, and other factors. Figure 8 shows the power output generated by the MPPT, showing minor fluctuations during the first 0.5 seconds before stabilizing at full capacity. The graph also displays the charging voltage, current received by the battery array, and the battery charge percentage over a 10-second simulation period. Additionally, simulating the circuit in Figure 5 allows for the observation of voltage levels and the charge percentage of the electric vehicle battery during the first 10 seconds, as shown in Figure 9.

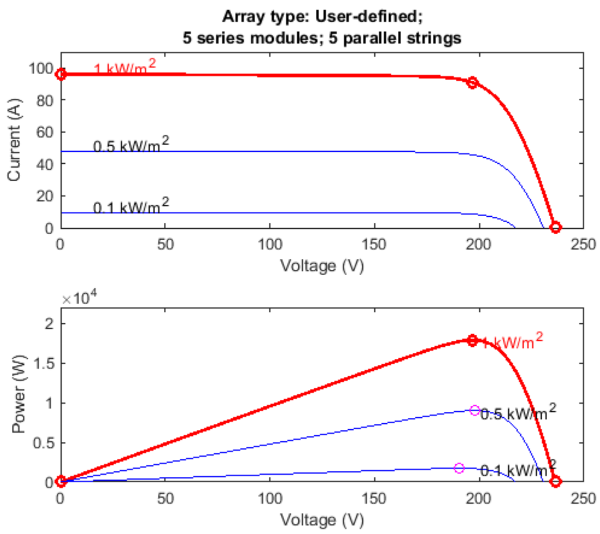

Figure 7. Power-to-current ratio based on solar irradiation

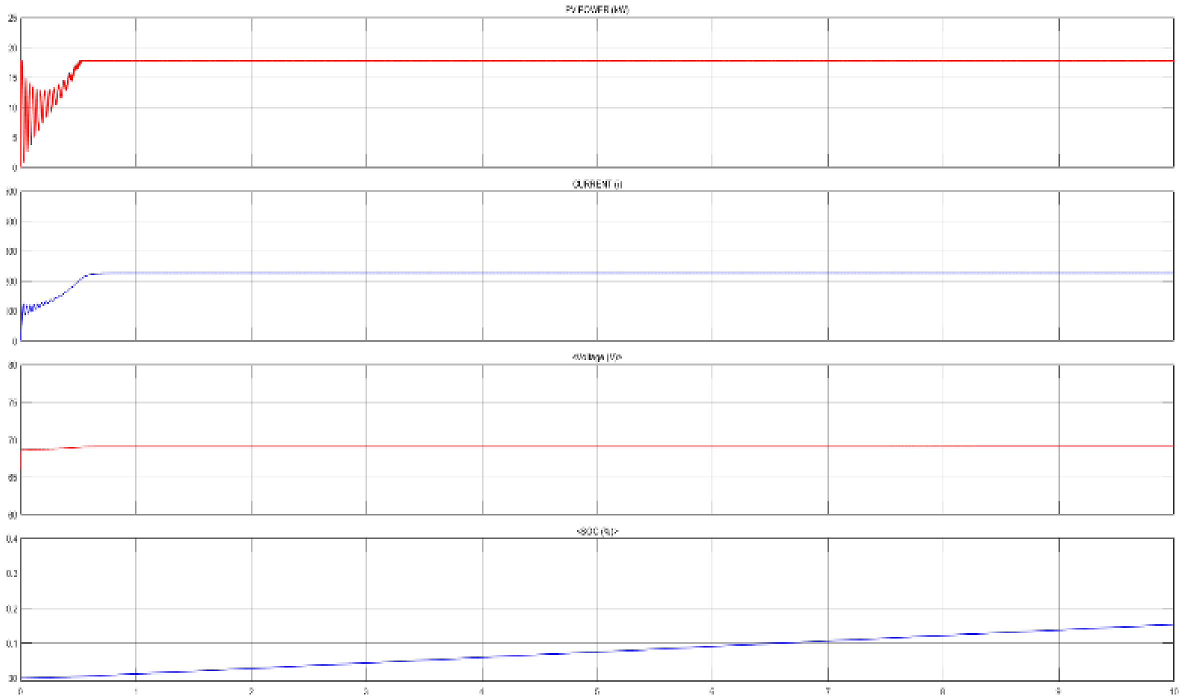

Figure 8. Charging system performance

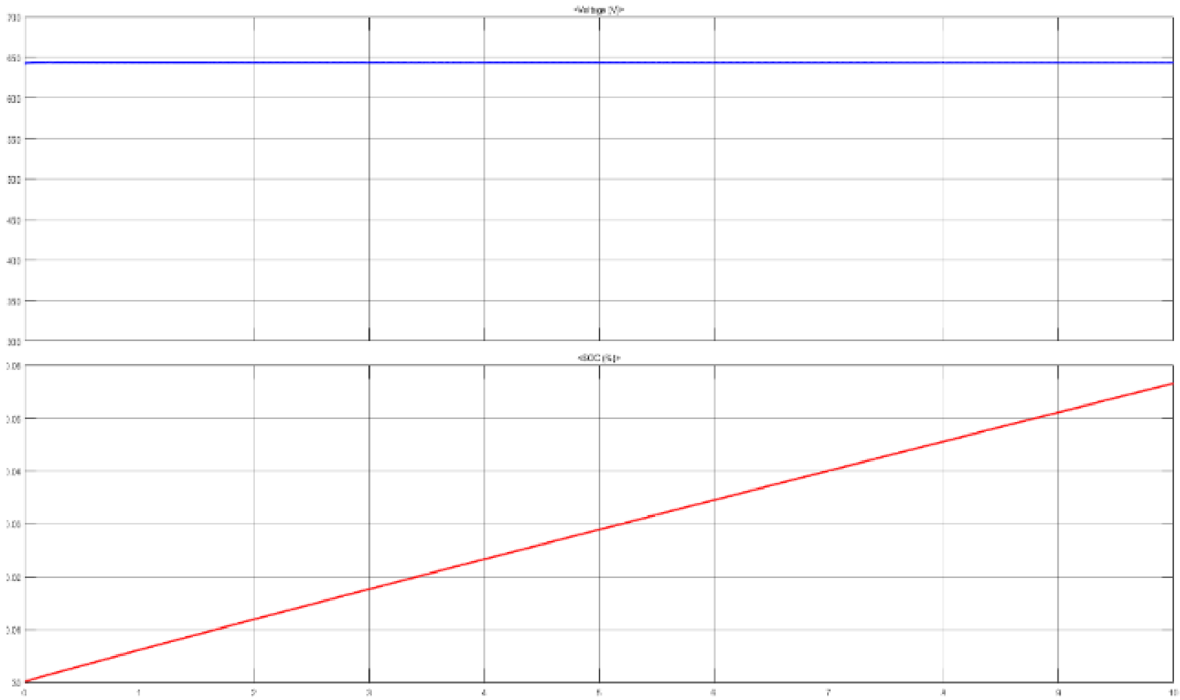

Figure 9. Electric vehicle charging graph

4. CONCLUSION

Results obtained show that designing an electric vehicle (EV) charging station requires selecting the appropriate AC or DC charging infrastructure. AC charging, though slower, remains the primary method in Colombia, while DC fast charging reduces charging time to under two hours, which is an important result. This means that future stations should prioritize DC charging to meet increasing demand, but AC chargers must still be included to accommodate existing vehicles. A hybrid charging station ensures accessibility and supports the transition to faster, more efficient charging solutions. The photovoltaic system's efficiency depends on available installation space and shading effects. The selected system requires 1,200 m² to install 260 solar panels, generating 184.47 kW_p, which is an important finding achieved in this project. Proper panel arrangement minimizes shading losses and maximizes solar energy output. Limited space may reduce the number of panels and affect power generation, emphasizing the need for optimal site assessment and layout planning.

For future projects it is important to know that initial investment for the charging station is approximately COP 772.9 million, but the return on investment (ROI) is only 2.8 years due to the low operating costs of solar energy. By generating 518.4 kWh of renewable energy, the system cuts electricity costs, reducing dependence on EMSA and fossil fuels. Additionally, the station's 1,000 kVA, 13,200 V transformers provide 800 kW, with a 20% power reserve for reliability. Over time, low operational expenses and high profitability make this a financially viable and sustainable solution.

ACKNOWLEDGEMENTS

The authors thank Universidad de los Llanos and Specialization in Instrumentation and Industrial Control for their support in the development of this project.

FUNDING INFORMATION

Product financed by the authors.

AUTHOR CONTRIBUTIONS STATEMENT

This journal uses the Contributor Roles Taxonomy (CRediT) to recognize individual author contributions, reduce authorship disputes, and facilitate collaboration.

Name of Author	C	M	So	Va	Fo	I	R	D	O	E	Vi	Su	P	Fu
Emerson Cabanzo Mosquera	✓	✓	✓	✓	✓	✓		✓	✓	✓			✓	✓
Walter Naranjo Lourido		✓	✓	✓	✓	✓	✓	✓	✓	✓	✓	✓	✓	✓
Javier Eduardo Martínez Baquero		✓		✓	✓	✓	✓			✓	✓	✓	✓	✓

C : **C**onceptualization
M : **M**ethodology
So : **So**ftware
Va : **Va**lidation
Fo : **Fo**rmal analysis
I : **I**nvestigation
R : **R**esources
D : **D**ata Curation
O : Writing - **O**riginal Draft
E : Writing - Review & **E**diting
Vi : **Vi**sualization
Su : **Su**pervision
P : **P**roject administration
Fu : **Fu**nding acquisition

CONFLICT OF INTEREST STATEMENT

Authors state no conflict of interest.

INFORMED CONSENT

Not applicable as it requires the involvement of personnel from outside the work team, no sensitive information was handled.

ETHICAL APPROVAL

Not applicable in the research.

DATA AVAILABILITY

The data that support the findings of this study are available from the corresponding author, JEMB, upon reasonable request.

REFERENCES

[1] R. Chen and Y. Kong, "A comprehensive review of greenhouse gas based on subject categories," *Science of The Total Environment*, vol. 866, p. 161314, 2023, doi: 10.1016/j.scitotenv.2022.161314.

[2] M. Tavassoli and A. Kamran-Pirzaman, "Comparison of effective greenhouse gases and global warming," in *2023 8th International Conference on Technology and Energy Management (ICTEM)*, 2023, pp. 1–5, doi: 10.1109/ICTEM56862.2023.10083954.

[3] S.-H. Liao, S. T. Tsai, and W.-L. Hsia, "Controlling and monitoring greenhouse gas emissions using CPS and GHG sensors," in *2023 IEEE 3rd International Conference on Electronic Communications, Internet of Things and Big Data (ICEIB)*, 2023, pp. 68–70, doi: 10.1109/ICEIB57887.2023.10170177.

[4] P. T. Aakko-Saksa *et al.*, "Reduction in greenhouse gas and other emissions from ship engines: Current trends and future options," *Progress in Energy and Combustion Science*, vol. 94, no. November 2022, 2023, doi: 10.1016/j.pecs.2022.101055.

[5] R. Huang and Z. Wang, "Prediction on Shanghai's energy consumption trend and carbon emission peak," in *2011 Third International Conference on Measuring Technology and Mechatronics Automation*, 2011, vol. 2, pp. 898–901, doi: 10.1109/ICMTMA.2011.507.

[6] L. Kniazkov, "Calculation of the radiative balance in a tropical atmosphere at different concentrations of carbon dioxide," in *2020 IEEE Ukrainian Microwave Week (UkrMW)*, 2020, pp. 776–780, doi: 10.1109/UkrMW49653.2020.9252815.

[7] W. Oelßner and J. Zosel, "CO2 measurement in biotechnology and industrial processes," in *Carbon Dioxide Sensing*, Wiley, 2019, pp. 349–365.

[8] S. M. Mojabi, M. Ghourchi, and F. Feizi, "Adverse consequences of conflicts and wars on environment and public health," in *2010 International Conference on Environmental Engineering and Applications*, 2010, pp. 125–129, doi: 10.1109/ICEEA.2010.5596109.

[9] J. Tan *et al.*, "Identify the risk of environmental degradation with ecological model and remote sensing: A case study of natural forest in xishuangbanna," in *2017 IEEE International Geoscience and Remote Sensing Symposium (IGARSS)*, 2017, pp. 3521–3524, doi: 10.1109/IGARSS.2017.8127758.

[10] Y. Yevdokimov, "Economic evaluation of climate chang impacts on road transportation in Atlantic Canada," in *2017 4th International Conference on Transportation Information and Safety (ICTIS)*, 2017, pp. 286–290, doi: 10.1109/ICTIS.2017.8047778.

[11] P. Hegyi, A. Jaber, D. Földes, B. Csonka, D. Silva, and C. Csiszár, "Assessing the impact of climate change and weather conditions endangering inland waterway navigation," in *2023 Smart City Symposium Prague (SCSP)*, 2023, pp. 1–5, doi: 10.1109/SCSP58044.2023.10146208.

[12] F. Farzaneh and S. Jung, "Lifecycle carbon footprint comparison between internal combustion engine versus electric transit vehicle: A case study in the U.S.," *Journal of Cleaner Production*, vol. 390, no. January, p. 136111, 2023, doi: 10.1016/j.jclepro.2023.136111.

[13] J. Archsmith, A. Kendall, and D. Rapson, "From cradle to junkyard: assessing the life cycle greenhouse gas benefits of electric vehicles," *Research in Transportation Economics*, vol. 52, pp. 72–90, 2015, doi: 10.1016/j.retrec.2015.10.007.

[14] S. Kosai, M. Nakanishi, and E. Yamasue, "Vehicle energy efficiency evaluation from well-to-wheel lifecycle perspective," *Transportation Research Part D: Transport and Environment*, vol. 65, pp. 355–367, 2018, doi: 10.1016/j.trd.2018.09.011.

[15] J. Morfeldt, S. D. Kurland, and D. J. A. Johansson, "Carbon footprint impacts of banning cars with internal combustion engines," *Transportation Research Part D: Transport and Environment*, vol. 95, no. May, 2021, doi: 10.1016/j.trd.2021.102807.

[16] R. Ramli, K. R. Purba, and I. Baydarova, "Preliminary study on the carbon footprint awareness & the analysis among university students in Malaysia," in *2024 20th IEEE International Colloquium on Signal Processing & Its Applications (CSPA)*, 2024, pp. 202–206, doi: 10.1109/CSPA60979.2024.10525357.

[17] N. D. Minh, H. M. Nguyet, and M. T. Hien, "Solar energy based charger station system for electric vehicle in Hanoi," in *2023 Asia Meeting on Environment and Electrical Engineering (EEE-AM)*, 2023, pp. 1–6, doi: 10.1109/EEE-AM58328.2023.10394753.

[18] P. Asopa, P. Purohit, R. R. Nadikattu, and P. Whig, "Reducing carbon footprint for sustainable development of smart cities using IoT," in *2021 Third International Conference on Intelligent Communication Technologies and Virtual Mobile Networks (ICICV)*, 2021, pp. 361–367, doi: 10.1109/ICICV50876.2021.9388466.

[19] Ministerio de Transporte, "Matrícula de vehículos eléctricos en el Registro Único Nacional de Tránsito (Runt)," *Ministerio de Transporte, Colombia*. [Online]. Available: https://mintransporte.gov.co/publicaciones/11015/colombia-tiene-8299-vehiculos-electricos-en-el-runt-1699-mas-de-la-meta-del-plan-nacional-de-desarrollo.

[20] Electromaps, "List of charging stations for electric vehicles in Colombia," *electromaps.com*. [Online]. Available: https://www.electromaps.com/en/charging-stations/colombia.

[21] Congreso de Colombia, "Ley 1964 de 2019: movilidad sostenible," *suin-juriscol.gov.co*, 2019, [Online]. Available: https://www.suin-juriscol.gov.co/viewDocument.asp?id=30036636#.

[22] EMSA, "Electrificadora del Meta." [Online]. Available: https://www.electrificadoradelmeta.com.co/search?query=TARIFAS.

[23] W. M. Najem, O. S. Alyozbaky, and S. M. Khudher, "Electric vehicles charging station configuration with closed loop control," *International Journal of Electrical and Computer Engineering (IJECE)*, vol. 13, no. 3, pp. 2428–2439, Jun. 2023, doi: 10.11591/ijece.v13i3.pp2428-2439.

[24] S. Naik, S. B. Bhoomika, S. Wali, H. M. Nikhita, M. Kappali, and A. R. Itagi, "Design and performance analysis of standalone solar PV based electric vehicle charging station," in *2023 IEEE North Karnataka Subsection Flagship International Conference (NKCon)*, 2023, pp. 1–6, doi: 10.1109/NKCon59507.2023.10396584.

[25] W. Liu, X. Wang, X. Zhang, Y. Ding, and Q. Li, "Design of detection and assessment system for electric vehicle charging station based on genetic algorithm," in *2023 International Conference on Power, Electrical Engineering, Electronics and Control (PEEEC)*, 2023, pp. 455–459, doi: 10.1109/PEEEC60561.2023.00094.

[26] F. R. A. Bukit, H. Zulkarnain, and C. P. Kusuma, "Optimizing electric vehicle charging station placement integrates distributed generations and network reconfiguration," *International Journal of Electrical and Computer Engineering*, vol. 14, no. 5, pp. 4929–4939, 2024, doi: 10.11591/ijece.v14i5.pp4929-4939.

[27] H. B. Tambunan *et al.*, "Initial location selection of electric vehicles charging infrastructure in urban city through clustering algorithm," *International Journal of Electrical and Computer Engineering*, vol. 13, no. 3, pp. 3266–3280, 2023, doi: 10.11591/ijece.v13i3.pp3266-3280.

[28] T. S. Biya and M. R. Sindhu, "Design and power management of solar powered electric vehicle charging station with energy storage system," in *2019 3rd International conference on Electronics, Communication and Aerospace Technology (ICECA)*, 2019, pp. 815–820, doi: 10.1109/ICECA.2019.8821896.

[29] S. Cho, J. Lim, W. Won, J. Kim, and S. Ga, "Design and optimization of energy supplying system for electric vehicles by mobile charge stations," *Journal of Industrial and Engineering Chemistry*, vol. 138, pp. 481–491, 2024, doi: 10.1016/j.jiec.2024.04.027.

[30] E. A. Mohammed, M. H. Qahtan, and A. J. Ali, "Internet of things based real-time electric vehicle and charging stations monitoring system," *Indonesian Journal of Electrical Engineering and Computer Science*, vol. 27, no. 3, pp. 1661–1669, 2022, doi: 10.11591/ijeecs.v27.i3.pp1661-1669.

[31] R. Gopalakrishnan, D. S. Vidhya, R. Gowshickraaj, E. Kamalakannan, and S. Narendran, "Design and implementation of roving charging station for electric vehicles," in *2023 7th International Conference on Trends in Electronics and Informatics (ICOEI)*, 2023, pp. 255–258, doi: 10.1109/ICOEI56765.2023.10125639.

[32] Y. Hakam, H. Ahessab, A. Gaga, M. Tabaa, and B. El Hadadi, "Design and simulation of a 5 KW solar-powered hybrid electric vehicle charging station with a ANN - Kalman filter MPPT and MPC-based inverter control for reduced THD," *Scientific African*, p. e02563, 2025, doi: 10.1016/j.sciaf.2025.e02563.

BIOGRAPHIES OF AUTHORS

Emerson Cabanzo Mosquera is a Mechatronics Engineer graduated from Universidad de Pamplona in 2020. Postgraduate in Instrumentation and Industrial Control at Universidad de los Llanos in 2023. Currently, he is employed as a mechatronics engineering instructor at TEINCO, with a particular focus on the domains of control and PLC. He can be contacted at email: emerson.cabanzo.mosquera@unillanos.edu.co.

Walter Naranjo Lourido received the B.S. degree in electronic engineering from Universidad Autonóma de Occidente, Cali, in 2005. Master's in engineering in Pontificia Universidad Javeriana de Cali in 2011 and PhD. Engineering from Universidad de los Andes, Bogotá in 2017. He was a postdoctoral research engineer at the Pontificia Universidad Católica, Santiago, Chile. He explores new power M2C topologies related to fast and ultra-fast DC chargers for electric vehicles. This research was funded by the National Agency of Research and Development (ANID) in Chile. His research interests are power electronics, vehicle electrification, design of powertrains, energy efficiency, and microgrids. His profile can be found at Research gate: https://www.researchgate.net/profile/Javier-Martinez-Baquero, Portal del Investigador: https://investigadores.anid.cl/es/public_search/researcher?id=22749. He can be contacted at email: wnaranjo@unillanos.edu.co.

Javier Eduardo Martinez Baquero is an electronic engineer graduate from Universidad de los Llanos in 2002. Posgraduated in Electronic Instrumentation from Universidad Santo Tomas in 2004, posgraduated in instrumentation and industrial control at Universidad de los Llanos in 2020 and MSc in educative technology and innovative media for Education at Universidad Autonoma de Bucaramanga in 2013. His current working as associated professor of Universidad de los Llanos and research focuses on instrumentation, automation, control and renewable energies. His profile can be found at Research gate: https://www.researchgate.net/profile/Javier-Martinez-Baquero. He can be contacted at email: jmartinez@unillanos.edu.co.